

# Interference Mitigation via Rate-Splitting and Common Message Decoding in Cloud Radio Access Networks

Alaa Alameer Ahmad<sup>\*</sup>, *Student Member, IEEE*, Hayssam Dahrouj<sup>†</sup>, *Senior Member, IEEE*, Anas Chaaban<sup>‡</sup>, *Senior Member, IEEE*,

Aydin Sezgin<sup>\*</sup>, *Senior Member, IEEE* and Mohamed-Slim Alouini<sup>§</sup>, *Fellow, IEEE*

## Abstract

Cloud-radio access networks (C-RAN) help overcoming the scarcity of radio resources by enabling dense deployment of base-stations (BSs), and connecting them to a central-processor (CP). This paper considers the downlink of a C-RAN, where the cloud is connected to the BSs via limited-capacity backhaul links. We propose and optimize a C-RAN transmission scheme that combines rate splitting, common message decoding, beamforming vectors design and clustering. To this end, the paper optimizes a transmission scheme that combines rate splitting (RS), common message decoding (CMD), clustering and coordinated beamforming. In this work we focus on maximizing the weighted sum-rate subject to per-BS backhaul capacity and transmit power constraints, so as to jointly determine the RS-CMD mode of transmission, the cluster of BSs serving private and common messages of each user, and the associated beamforming vectors of each user private and common messages. The paper proposes solving such a complicated non-convex optimization problem using  $l_0$ -norm relaxation techniques, followed by inner-convex approximations (ICA), so as to achieve stationary solutions to the relaxed non-convex problem. Numerical results show that the proposed method provides significant performance gain as compared to conventional interference mitigation techniques in C-RAN which simply treat interference as noise (TIN).

Part of this paper was presented at the IEEE International Workshop on Signal Processing Advances in Wireless Communications (SPAWC), Kalamata, Greece, June 2018 [1].

A. A. Ahmed and A. Sezgin are with the Department of Electrical Engineering Ruhr-university Bochum, Germany (Email: {alaa.alameerahmad, aydin.sezgin}@rub.de). H. Dahrouj is with the Department of Electrical and Computer Engineering, Effat University, Saudi Arabia (Email: hayssam.dahrouj@kaust.edu.sa). A. Chaaban is with the School of Engineering, The University of British Columbia, Kelowna, Canada (Email: anas.chaaban@ubc.ca). M. S. Alouini is with the Communication Theory Lab, King Abdullah University of Science and Technology, Thuwal, Saudi Arabia (Email: slim.alouini@kaust.edu.sa).

## I. INTRODUCTION

### A. Overview

Motivated by the scarcity of radio resources and the ever increasing need for higher data rates and reliable wireless services, C-RAN provides a practical network architecture capable of boosting the spectral and energy efficiency in next generation wireless systems (5G and beyond) [2]–[4]. By connecting many BSs to the CP, C-RANs enable spatial reuse through dense deployment of small cells, and exploit the emerging cloud-computing technologies for managing large networks [5], [6].

With ultra dense deployment of small cells, the distance between the base station (BS) and the end user decreases, which results in a better quality of the direct channel. This comes, however, at the cost of increasing inter-BS interference due to proximity of the BSs in neighbouring cells. Furthermore, in C-RAN, the performance of the system is also limited by the finite capacity of backhaul links, [7]–[13]. Intuitively, in the extreme case when the backhaul capacity goes to infinity, the C-RAN is equivalent to a broadcast channel (BC). In the other extreme in which the backhaul links have zero-capacity, the C-RAN becomes equivalent to an interference channel (IC), the capacity of which is still a well-known open problem, even for the simple two-user IC, where treating interference as noise (TIN) is known to be a suboptimal strategy, especially in high-interference regimes [14]–[17]. With limited backhaul capacity, C-RAN bridges the two extremes. With this observation in mind, we investigate in this paper a transmission scheme which improves the performance of C-RAN in different regimes, i.e., in backhaul limited regimes and interference limited regimes.

In the rate splitting strategy, initially introduced by [14] for the IC, the message of each user is split into two parts: a private part decodable at the intended user only and a common part which can be decoded by other user. Such a strategy is shown to approach the capacity region of the IC in the seminal works of [15], [16]. Motivated by this fact, this paper studies rate-splitting in the realm of a C-RAN. It proposes splitting the message of each user into two parts, a private part decodable at the intended user only, and a common part which can be decoded at a subset of users.

Since the CP is connected to the BSs in cloud-enabled networks, C-RAN becomes a particularly suitable platform for the physical implementation of rate-splitting strategies. In the context of our paper, all rate splitting and common message decoding (RS-CMD) techniques are adopted

for the sole purpose of reducing large-scale interference. As the CP is connected to the BSs via finite capacity backhaul links, it becomes equally important to determine the set of BSs (i.e., cluster) which serves each user, jointly with selecting the mode of transmission of each user (i.e., private, common, or both).

This work considers the RS-CMD problem in the downlink of a C-RAN, where the CP is connected to several BSs, each equipped with multiple antennas. The CP applies central encoding to user's messages and establishes cooperation between a cluster of BSs by joint design of linear precoding in a user-centric clustering fashion, also known as *data-sharing* strategy [18]–[21], as it achieves a better performance compared to classical transmission schemes [22]. The paper then considers the problem of maximizing the weighted sum-rate (WSR) across the network, subject to per-BS backhaul capacity and transmission power constraints. The goal of this optimization is to jointly determine the RS-CMD mode of transmission, the cluster of BSs serving private and common messages of each user, and the associated beamforming vectors of each user private and common information. The paper provides an in-depth numerical investigation of the impact of RS-CMD strategy on the achievable rate in C-RANs, and compares it with the conventional strategies which treat interference as noise.

## B. Related Work

The contributions of this paper are related to works on rate splitting and common message decoding, clustering, and beamforming; topics which are studied in the literature of wireless systems, both individually and separately.

In rate-splitting schemes, the data of each user is divided into two parts: a private message which is decoded only at the intended user, and a common message which is decodable at the intended user and a subset of the unintended users. Reference [15] shows that such a RS-CMD technique leads to the largest known achievable rate-region in a 2-user IC. Such splitting strategy is further shown in [16] to achieve rates within one-bit from the capacity of the 2-user IC. Although being based on simple networks, those information-theoretical studies show the benefits of using RS-CMD techniques in high interference regimes. For instance, inspired by the theoretical works in [15], [16], the authors in [23] generalize this RS-CMD scheme to a practical multi-cell network showing significant achievable rate improvement by jointly designing the beamforming vectors for private and common information in RS-CMD as compared to beamforming design using TIN. In [24], the authors apply RS ideas to a practical setup of

heterogeneous wireless networks. The results in [24] suggest that a significant performance gain can be reached by applying RS as compared to rank-1 coordinated beamforming schemes that adopt TIN strategy. The work in [25] uses common message decoding and successive interference cancellation techniques to maximize the sum rate in multi-cell multi-user MIMO system. The difference of convex optimization technique is used to efficiently solve the difficult underlying optimization problem. Recently, RS-CMD has also gained a noteworthy attention in the literature of medium access schemes. For instance, the authors in [26] propose a novel RS multiple access (RSMA) scheme, which generalizes and outperforms conventional multiple access schemes such as Space-Division Multiple Access (SDMA) and Non-Orthogonal Multiple Access (NOMA). Based on these results, the authors in [27] show that RSMA is more energy efficient than SDMA and NOMA. Reference [28], on the other hand, shows that linearly precoded RS is more efficient than the conventional Multi-User Linear Precoding (MU-LP) in terms of spectral and energy efficiency. Through numerical simulations, the authors in [28] particularly show that, with no increase in receiver complexity, RS achieves better performance metrics as compared to both NOMA and MU-LP systems. The above works, i.e., [15], [16], [23]–[28], however, do not address cloud-enabled scenarios, as they ignore the physical-layer considerations induced by RS-CMS in C-RANs, and do not account for determining the set of common messages. This paper, therefore, focuses on the study of the joint resource allocation problem in C-RAN, together with evaluating the impact of RS-CMD techniques. The paper further develops a well-chosen heuristic procedure to determine the set of common messages that each user needs to decode.

In general, most of the existing works (e.g., [29]–[34]) on multi-cell interference mitigation in practical networks focus on doing so through jointly allocating resources (e.g., beamforming vectors and transmit power) in order to maximize a network utility. References [29]–[34], however, often adopt the strategy of TIN and assume an infinite backhaul capacity. Towards this end, the impact of finite backhaul links capacity is studied in the downlink of C-RAN in [21]. The problem studied in [21] turns out to be a mixed-integer non linear problem (MINLP), which is solved by relaxing the discrete non-convex per-BS backhaul constraints using re-weighted  $l_1$ -norm, and then by applying a generalized weighted minimum mean square algorithm (WMMSE). The authors in [7] consider the joint design of BSs' clusters and beamforming vectors to minimize the network-wide transmit power cost. The trade-off between the backhaul traffic and transmit power is also investigated in references [9]–[13], [21], all of which adopt TIN to decode the received messages. At this point, it becomes essential to investigate how adopting RS-CMD can

influence the design of clusters of BSs and the beamforming vectors associated with the private and common messages in a C-RAN setup. Towards this end, our current paper investigates the downlink C-RAN by utilizing a RS-CMD strategy, and focuses on evaluating its impact on jointly optimizing the beamforming vectors, the clustering and the transmission mode, so as to maximize the weighted-sum rate (WSR) across the network. To the best of authors' knowledge, this is the first work on C-RAN which studies both the application of RS-CMD coupled with joint clustering and beamforming, and numerically illustrates the potential gain provided by RS-CMD over TIN.

### C. Contributions

In this paper, we propose using RS-CMD in downlink C-RAN to jointly design user centric clusters of BSs, so as to explore RS-CMD benefits in large-scale interference management. We formulate a WSR maximization problem subject to per-BS backhaul capacity and per-BS transmit power constraints, so as to determine the RS splitting mode, the cluster of BSs which serves each user, and the beamforming vectors associated with the private and common messages parts. Such a problem is generally NP-hard due to its mixed discrete and continuous optimization nature, in addition to the non-convexity of the constraints. Our paper proposes solving such a problem using a heuristic based on  $l_0$ -norm approximation to tackle the discrete part, followed by a polynomial time algorithm based on inner convex approximations, so as to find a stationary solution to the resulting non-convex continuous problem. The paper subsequently shows the numerical benefits of the proposed RS-CMD scheme in improving the achievable rates in C-RAN compared to the state-of-the art TIN strategy, both in the backhaul-limited and in the interference-limited regimes. Our main contributions can be summarized as follows:

- *Common Message Decoding (CMD) Set*: We propose a heuristic procedure for ordering the set of strongest interferers for each user, which consequently allows for determining the set of common messages to be decoded.
- *Clustering*: Based on  $l_0$ -norm relaxation and inner-convex approximation framework, we propose a dynamic clustering approach. In the context of RS-CMD, we determine the set of BSs serving the private message and the set of BSs which serves the common message for each scheduled user. As opposed to the static clustering scheme described in [21], dynamic clustering procedure forms the clusters by taking into account the CMD set of each user, which can significantly affect the network connectivity. To deal with the non-

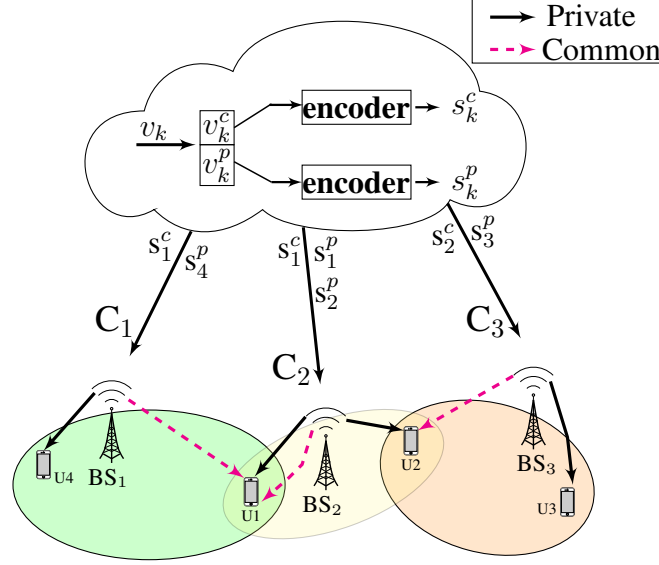


Figure 1: A C-RAN system with three cells. Both private and common messages are designed at the cloud.

convex backhaul constraint, the paper particularly proposes a surrogate convex function to approximate the backhaul constraint. The paper then compensates for such approximations using proper outer-loop updates in an iterative manner.

- *Beamforming*: Even when the clusters are fixed, the WSR problem with RS-CMD is not convex. This is because the private and common rate functions are non-convex in the private and common beamforming vectors, respectively. The paper, therefore, proposes solving such issue using an algorithm that applies well-chosen inner-convex approximations. The proposed algorithm is proven to converge in polynomial time to a stationary solution.
- *Numerical Simulations*: We show through extensive numerical simulations that our proposed solution outperforms the classical TIN in C-RAN. In both the interference limited and the backhaul limited regimes, we illustrate that RS-CMD makes a better use of the network resources in order to achieve higher rates as compared with TIN for different network parameters.

The rest of the paper is organized as follows. Section II illustrates the system model. Section III introduces the transmission scheme adopted in this work and formulates the WSR problem accordingly. The proposed solution is introduced in section IV. Section V presents the numerical simulations, and section VI concludes the paper.

## II. SYSTEM MODEL

We consider a C-RAN system operating in downlink mode with a transmission bandwidth  $B$ . The network consists of a set of multi-antenna BSs  $\mathcal{N} = \{1, 2, \dots, N\}$ , serving a set of single-antenna users  $\mathcal{K} = \{1, 2, \dots, K\}$ . Each BS is equipped with  $L \geq 1$  antennas. BS  $n \in \mathcal{N}$  is connected to a CP, located at the cloud, via a backhaul link of capacity  $C_n$ . User  $k$  requires a message  $v_k$ , where the achievable data-rate at user  $k$  is denoted by  $R_k$ . All messages are jointly encoded at the CP into signals  $s_k$ ,  $\forall k \in \mathcal{K}$ . The CP then shares combinations of  $s_k$  (or parts thereof) with the BSs through the backhaul links. This data-sharing is possible if the rate of signals shared with BS  $n$  does not exceed the backhaul capacity  $C_n$ . This is made more explicit when we describe RS in the next section. Upon receiving these signals, BS  $n$  constructs  $\mathbf{x}_n \in \mathbb{C}^{L \times 1}$ , and sends it according to the following transmit power constraint:

$$\mathbb{E} \{ \mathbf{x}_n^H \mathbf{x}_n \} \leq P_n^{\text{Max}} \quad \forall n \in \mathcal{N}, \quad (1)$$

where  $P_n^{\text{Max}}$  is the maximum transmit power available at BS  $n$ .

Let  $\mathbf{h}_{n,k} \in \mathbb{C}^{L \times 1}$  denote the channel vector between BS  $n$  and user  $k$ , and  $\mathbf{h}_k = [\mathbf{h}_{1,k}^T, \mathbf{h}_{2,k}^T, \dots, \mathbf{h}_{N,k}^T]^T \in \mathbb{C}^{NL \times 1}$  be the aggregate channel vector of user  $k$ . We can write the received signal at user  $k$  as

$$y_k = \mathbf{h}_k^H \mathbf{x} + n_k \quad (2)$$

where  $n_k \sim \mathcal{CN}(0, \sigma^2)$  is the additive white Gaussian noise (AWGN), and  $\mathbf{x} = [\mathbf{x}_1^T, \dots, \mathbf{x}_N^T]^T$ .

For mathematical tractability, the paper assumes that the CP has complete knowledge of the instantaneous channel state information (CSI) of all BSs. We further adopt a block-based transmission model, where each transmission block consists of several time slots. The channel fading coefficients remain constant within one block, but may vary independently from one block to another. Next, we describe our proposed scheme which is based on RS-CMD, and we formulate the WSR optimization problem accordingly.

## III. TRANSMISSION SCHEME AND PROBLEM FORMULATION

The proposed transmission scheme consists of RS, joint beamforming and data-sharing, and successive common message decoding. We start by describing RS.

### A. Rate Splitting

The CP first splits the message of user  $k$ , i.e.,  $v_k$ , into a private message denoted by  $v_k^p$ , and a common message denoted by  $v_k^c$ . Afterwards, the CP encodes the private and common messages into  $s_k^p$  and  $s_k^c$ , respectively, as illustrated in Fig. 1. The coded messages  $s_k^p$  and  $s_k^c$  are assumed to be i.i.d. circularly symmetric complex Gaussian with zero mean and unit variance. Their respective rates are denoted by  $R_k^p$  and  $R_k^c$ , and so  $R_k = R_k^p + R_k^c$ , where  $R_k$  is the rate of user  $k$ .

### B. Beamforming, Signal Construction, and Data-Sharing

When adopting the data-sharing strategy in a downlink mode in C-RAN which applies RS-CMD, the CP shares the encoded private and common messages directly with their respective cluster of BSs. Let  $\mathcal{K}_n^p, \mathcal{K}_n^c \subseteq \mathcal{K}$  be the subset of users served by BS  $n$  with a private or common message, respectively, i.e.,

$$\mathcal{K}_n^p := \{k \in \mathcal{K} \mid \text{BS } n \text{ delivers } s_k^p \text{ to user } k\}, \quad (3)$$

$$\mathcal{K}_n^c := \{k \in \mathcal{K} \mid \text{BS } n \text{ delivers } s_k^c \text{ to user } k\}. \quad (4)$$

Moreover, let the beamformers used by BS  $n$  to send  $s_k^p$  and  $s_k^c$  to user  $k$  be denoted by  $\mathbf{w}_{n,k}^p$  and  $\mathbf{w}_{n,k}^c$ , respectively. Then, the CP sends  $\{s_k^p \mid \forall k \in \mathcal{K}_n^p\}$ ,  $\{s_k^c \mid \forall k \in \mathcal{K}_n^c\}$  and their beamforming vectors over the backhaul links to BS  $n$ . Due to the finite backhaul capacity  $C_n$  limits, the transmission rate is subject to the following backhaul capacity constraint<sup>1</sup>:

$$\sum_{k \in \mathcal{K}_n^p} R_k^p + \sum_{k \in \mathcal{K}_n^c} R_k^c \leq C_n, \quad \forall n \in \mathcal{N} \quad (5)$$

BS  $n$  then constructs  $\mathbf{x}_n$  as follows:

$$\mathbf{x}_n = \sum_{k \in \mathcal{K}_n^p} \mathbf{w}_{n,k}^p s_k^p + \sum_{k \in \mathcal{K}_n^c} \mathbf{w}_{n,k}^c s_k^c. \quad (6)$$

Using the expression of the transmit signal (6), one can rewrite the power constraint (1) as follows:

$$\sum_{k \in \mathcal{K}} \left( \|\mathbf{w}_{n,k}^p\|_2^2 + \|\mathbf{w}_{n,k}^c\|_2^2 \right) \leq P_n^{\text{Max}}, \quad \forall n \in \mathcal{N}. \quad (7)$$

<sup>1</sup>We ignore the overhead due to sending the beamformers since these need to be sent only when CSI changes.



The private (common) message of user  $k$  is served by BS  $n$ , if the corresponding beamforming vector  $\mathbf{w}_{n,k}^p$  ( $\mathbf{w}_{n,k}^c$ ) is non-zero. This can be equivalently expressed in terms of the indicator function as follows:

$$\mathbb{1} \left\{ \|\mathbf{w}_{n,k}^o\|_2^2 \right\} = \begin{cases} 1 & \text{if } \|\mathbf{w}_{n,k}^o\|_2^2 > 0 \\ 0 & \text{otherwise} \end{cases} \quad (8)$$

where,  $o \in \{p, c\}$ . Without loss of generality, the above indicator function can be written as a function of an  $l_0$ -norm notation<sup>2</sup>, i.e., as  $\mathbb{1} \left\{ \|\mathbf{w}_{n,k}^o\|_2^2 \right\} = \left\| \|\mathbf{w}_{n,k}^o\|_2^2 \right\|_0$ . This is this case since, in the scalar case, the  $l_0$ -norm definition coincides with the definition of the indicator function, because the power transmitted from BS  $n$  to user  $k$  is a positive scalar, i.e.,  $\|\mathbf{w}_{n,k}^o\|_2^2 \in \mathbb{R}_+$ . The subset of users served with private and common messages from BS  $n$  can, therefore, be expressed as:

$$\mathcal{K}_n^p = \left\{ k \mid \left\| \|\mathbf{w}_{n,k}^p\|_2^2 \right\|_0 = 1 \right\}, \quad (9)$$

$$\mathcal{K}_n^c = \left\{ k \mid \left\| \|\mathbf{w}_{n,k}^c\|_2^2 \right\|_0 = 1 \right\}. \quad (10)$$

The above expressions allow to re-express the backhaul constraint (5) in the following compact form:

$$\sum_{k \in \mathcal{K}} \left( \left\| \|\mathbf{w}_{n,k}^p\|_2^2 \right\|_0 R_k^p + \left\| \|\mathbf{w}_{n,k}^c\|_2^2 \right\|_0 R_k^c \right) \leq C_n, \quad \forall n \in \mathcal{N}. \quad (11)$$

### C. Successive Decoding

At this step, the received signal at user  $k$  can be written as

$$y_k = \mathbf{h}_k^H (\mathbf{w}_k^p s_k^p + \mathbf{w}_k^c s_k^c) + \sum_{j \in \mathcal{K} \setminus \{k\}} \mathbf{h}_k^H (\mathbf{w}_j^p s_j^p + \mathbf{w}_j^c s_j^c) + n_k,$$

where  $\mathbf{w}_k^p = [(\mathbf{w}_{1,k}^p)^T, \dots, (\mathbf{w}_{N,k}^p)^T]^T$  is the aggregate beamforming vector associated with  $s_k^p$ , i.e., the private message of user  $k$ . Similarly,  $\mathbf{w}_k^c$  is the aggregate beamforming vector associated with  $s_k^c$ , i.e., the common message of user  $k$ .

In the context of this paper, using common messages is adopted for the sole purpose of mitigating interference in C-RANs. Thus, the order in which user  $k$  decodes the intended

<sup>2</sup> $l_0$ -norm of a vector is the number of non-zero elements in this vector.

messages plays an important role in assessing the efficiency of the relevant proposed interference mitigation techniques. Although joint decoding of all common and private messages at user  $k$  would result in optimized rates, its implementation is complicated in practice, in particular when the network and the intended set of messages to be decoded by each user are large. The classical information theoretical results of a 2-user IC, however, already suggest that decoding a strong interferer's common message can significantly improve a user's achievable rate [16]. From this perspective, in this paper, we focus on a successive decoding strategy, wherein user  $k$  decodes a subset of all common messages in a fixed decoding strategy, based on the descending order of the channel gains of the interferers, as described next.

Let  $\mathcal{M}_k$  denote the set of users which decode  $s_k^c$ , i.e.:

$$\mathcal{M}_k := \{j \in \mathcal{K} \mid \text{user } j \text{ decodes } s_k^c\}. \quad (12)$$

The set of common messages that user  $k$  would decode is then defined as:

$$\Phi_k := \{j \in \mathcal{K} \mid k \in \mathcal{M}_j\}. \quad (13)$$

We note that once the set  $\mathcal{M}_k$  is found, we can determine the set  $\Phi_k$ , and vice-versa. The choice of  $\Phi_k$  (and consequently  $\mathcal{M}_k$ ) has a crucial impact on the achievable rate of user  $k$ . In this paper, we design  $\Phi_k$  (and  $\mathcal{M}_k$ ) in a heuristic fashion, which is based on the order of the interfering channel gains.

Consider the following decoding order at user  $k$ :

$$\pi_k(j) : \{1, 2, \dots, |\Phi_k|\} \rightarrow \Phi_k,$$

which represents a permutation of an ordered set with cardinality of  $|\Phi_k|$ , i.e.,  $\pi_k(j)$  is the successive decoding step in which the message  $j \in \Phi_k$  is decoded at user  $k$ . In other terms,  $\pi_k(j_1) > \pi_k(j_2)$  (where  $j_1 \neq j_2$ ) implies that user  $k$  decodes the common message of user  $j_1$  first, and then the common message of user  $j_2$ . Now, write  $\mathbf{y}_k$ , the received signal at user

$k$ , as follows,

$$\begin{aligned}
 y_k = & \underbrace{\left( \mathbf{h}_k^H \mathbf{w}_k^p s_k^p + \sum_{j \in \Phi_k} \mathbf{h}_k^H \mathbf{w}_j^c s_j^c \right)}_{\text{Signals to be decoded}} \\
 & + \underbrace{\sum_{j \in \mathcal{K} \setminus k} \mathbf{h}_k^H \mathbf{w}_j^p s_j^p + \sum_{l \in \mathcal{K} \setminus \Phi_k} \mathbf{h}_k^H \mathbf{w}_l^c s_l^c}_{\text{Interference plus noise}} + n_k.
 \end{aligned} \tag{14}$$

Since finding the optimal decoding order is obviously a challenging problem for its combinatorial nature, we herein propose a practical successive decoding strategy instead. The idea is to fix the decoding order according to channel strength in descending order as follows:  $\|\mathbf{h}_{\pi_k(1)}\| \geq \|\mathbf{h}_{\pi_k(2)}\| \geq \dots \geq \|\mathbf{h}_{\pi_k(|\Phi_k|)}\|$ . Such decoding strategy helps the users whose common messages are decoded achieving better common rates. Although the proposed decoding technique does not provide the global optimal solution to the problem, the simulations section of the paper later illustrate how that such a decoding order indeed provides an appreciable gain as compared to the conventional private-information transmission only, i.e., TIN.

#### D. Achievable Rate

Let  $\Gamma_k^p, \Gamma_{k,i}^c$  denote the signal to interference plus noise ratios (SINR's) of user  $k$ , when decoding its private message and the common message of user  $i$ , respectively. Based on equation (14), we can write:

$$\Gamma_k^p = \frac{|\mathbf{h}_k^H \mathbf{w}_k^p|^2}{\sum_{j \in \mathcal{K} \setminus k} |\mathbf{h}_k^H \mathbf{w}_j^p|^2 + \sum_{l \in \mathcal{K} \setminus \Phi_k} |\mathbf{h}_k^H \mathbf{w}_l^c|^2 + \sigma^2} \tag{15}$$

$$\Gamma_{k,i}^c = \frac{|\mathbf{h}_k^H \mathbf{w}_i^c|^2}{T_k + \sum_{l \in \mathcal{K} \setminus \Phi_k} |\mathbf{h}_k^H \mathbf{w}_l^c|^2 + \sum_{\substack{m \in \Phi_k \\ \pi_k(m) > \pi_k(i)}} |\mathbf{h}_k^H \mathbf{w}_m^c|^2} \tag{16}$$

where  $T_k = \sum_{j \in \mathcal{K}} |\mathbf{h}_k^H \mathbf{w}_j^p|^2 + \sigma^2$ . The above expressions (15) and (16) assume that each user decodes its private message last, which is adopted for its capability to reduce the interference through common message decoding, as in the classical multi-cell systems [23]. The total achiev-

able rate of user  $k$ ,  $R_k = R_k^p + R_k^c$ , then satisfies the following achievability conditions:

$$\Gamma_k^p \geq 2^{R_k^p/B} - 1, \quad \forall k \in \mathcal{K}, \quad (17)$$

$$\Gamma_{i,k}^c \geq 2^{R_k^c/B} - 1, \quad \forall i \in \mathcal{M}_k \text{ and } \forall k \in \mathcal{K}. \quad (18)$$

### E. Determining the Common Message Sets

The latest results of TIN in interference networks, e.g., [35], suggest a scheduling procedure to manage interfering links in a device-to-device (D2D) network. The idea in [35] is to allow the links which meet the TIN optimality criteria to share the same resources block (bandwidth, transmit frequency). Optimality of TIN criteria is then illustrated in terms of generalized degrees-of-freedom. In short, if a link causes much interference to other links (already scheduled to a transmitting resource block), or suffers from much interference, then one should schedule it to another block.

In the context of our paper, instead of scheduling users to other transmitting blocks, we propose to deploy RS-CMD strategy for the users which cause high levels of interference to other users, so as to determine a heuristic, yet reasonable, strategy for determining the common message sets. To this end, we propose a simple criterion to identify the users which receive too much interference (weak users), and allow them to decode the common messages of strong interferers (strong users). The network we are interested in is more complex than those studied in [35]–[37]. The proposed criterion, although being a heuristic one, leads to a significant gain over the TIN strategy used in the state-of-the art C-RAN, as illustrated later in the simulations section.

Our proposed algorithm relies on first identifying the users for which TIN is not optimal, i.e., solely based on their channel gains. We do so by initializing the beamformers of all users as feasible maximum ratio combining (MRC) beamformers. Then we compute the achievable rates, and for each user, we evaluate the total interference received from other users. To best identify whether a user is considered as a weak or a strong interferer, we define a parameter  $\mu$  as a separating threshold. More specifically, if the rate of a user  $k$  is within the  $\mu$ th percentile, the user is considered a weak user, and up to  $D$  strongest interferers of user  $k$  are added to the set  $\Phi_k$ . Here,  $D$  represents the number of layers in successive decoding strategy. We note that  $\mu$  plays an important role in bridging the gap between RS with RS-CMD. In other terms, when  $\mu$  is small, only the weakest users would decode the common message of their interferers. By increasing  $\mu$ , however, more users participate in decoding the common messages of their interferers. The value

of  $\mu$  plays an important role in determining the gain of RS-CMD over TIN as the simulations results later suggest.

The above strategy guarantees that user  $k$  would mitigate the interference it receives by decoding the common message of the strongest interferer. The intuition behind this is that, if the rate of a user  $k$  is high relative to other weakest users, this user would not be receiving a high level of interference, which makes it less useful that user  $k$  would decode the common message of other users. The steps of determining the set of common messages for all users  $k \in \mathcal{K}$  are summarized in Algorithm 1 description below.

---

**Algorithm 1** Procedure to Identify  $\{\Phi_k\}_{k=1}^K$

---

- 1: **Input:** CSI matrix  $\mathbf{H}$ , set of active users  $\mathcal{K}$  and initialize  $\{\Phi_k = \{k\}\}_{k=1}^K$ .
  - 2: Compute the beamformers as  $\mathbf{W} = \mathbf{H}^H$ .
  - 3: Compute the achievable rates using TIN, based on step 2,.
  - 4: **for**  $k \in \mathcal{K}$  **do**
  - 5:    $\hat{\mathcal{K}} \leftarrow \mathcal{K} \setminus \{k\}$
  - 6:   Compute the interference power  $\{I_{k,i}\}_{i \in \hat{\mathcal{K}}}$  as observed at user  $k$ .
  - 7:
  - 8:   **if**  $R_k$  is within the  $\mu$ -th percentile of other users rate **then**
  - 9:      $\Phi_k = \Phi_k \cup \left\{ \underset{i \in \hat{\mathcal{K}}}{\operatorname{argmax}} I_{k,i} \right\}$
  - 10:     $\hat{\mathcal{K}} \leftarrow \hat{\mathcal{K}} \setminus \left\{ \underset{i \in \hat{\mathcal{K}}}{\operatorname{argmax}} I_{k,i} \right\}$
  - 11:    **if**  $|\Phi_k| > L$  **then**
  - 12:      $\mathcal{K} \leftarrow \mathcal{K} \setminus \{k\}$
  - 13:    **end if**
  - 14:   **end if**
  - 15: **end for**
- 

#### F. Problem Formulation

The optimization problem considered in this paper focuses on maximizing the weighted sum-rate (WSR) in RS-CMD C-RAN. The goal is to determine the common and private beamformers jointly with the common and private clusters of BSs associated with each user, subject to per BS transmission power and backhaul constraints. The considered WSR maximization problem

can be mathematically written as:

$$\begin{aligned} & \underset{\{\mathbf{w}_k^p, \mathbf{w}_k^c | \forall k \in \mathcal{K}\}}{\text{maximize}} && \sum_{k=1}^K \alpha_k (R_k^p + R_k^c) \end{aligned} \quad (19a)$$

$$\text{subject to} \quad (7), (11) \quad (19b)$$

$$\Gamma_k^p \geq 2^{R_k^p/B} - 1 \quad \forall k \in \mathcal{K} \quad (19c)$$

$$\Gamma_{i,k}^c \geq 2^{R_k^c/B} - 1 \quad \forall i \in \mathcal{M}_k \text{ and } \forall k \in \mathcal{K} \quad (19d)$$

where the coefficient  $\alpha_k$  refers to the priority weight associated with user  $k$ . Problem (19) is a mixed integer non linear problem, which is generally an NP-hard problem, due to its mixed discrete and continuous optimization nature, and the non-convexity of the underlying objective and constraints as a function of the beamforming vectors. To tackle this challenging problem, we propose an iterative algorithm based on a strongly inner-convex approximation framework coupled with a smooth approximation of the non-smooth, non-convex  $l_0$ -norm. Before we proceed to the technical details of our approach, we elaborate on the structure of problem (19). The problem is non-convex even if we relax the binary constraints in (11), e.g., by using  $l_1$  relaxation to the  $l_0$ -norm. This is due to non-convexity of the objective (19a) as a function of the beamforming vectors. Moreover, the achievability constraints and the backhaul constraints in (19c)-(19d) and (11) are non-convex functions, and define a non-convex feasible set. To overcome this difficulty, we approximate each non-convex function with a surrogate upper-bound convex function, which helps approximating the non-convex feasible set with a convex one. Then, we iteratively refine this approximation till convergence. The following section describes all the technicalities of the above steps in details.

#### IV. PROPOSED SOLUTION

In this section, we present our proposed framework to tackle problem (19). We start by relaxing the discrete variables, and then we proceed by introducing an inner convex approximation (ICA) reformulation of the non-convex clustering problem. After determining the clusters, we determine the optimal beamforming vectors and the RS mode to transmit private and common messages, respectively, which also quantifies how much rate is assigned to the private and common messages, respectively.

### A. Relaxing the $l_0$ -norm

We use a smooth concave function to approximate the non-smooth, non-convex (in fact integer)  $l_0$ -norm. Consider the function  $f_\theta(x)$  defined as:

$$f_\theta(x) = \frac{2}{\pi} \arctan\left(\frac{x}{\theta}\right), \quad x \geq 0 \quad (20)$$

which is often used in the literature to approximate the  $l_0$ -norm [10], [38]. Here,  $\theta$  is a smoothness parameter which controls the quality of the  $l_0$ -norm approximation. After relaxing the discrete  $l_0$ -norm, we reformulate the problem (19) by introducing SINR variables instead of using the rate expressions. Let  $R_k^p = B \log_2(1 + \gamma_k^p)$  and  $R_k^c = B \log_2(1 + \gamma_k^c)$  for some  $\gamma_k^p, \gamma_k^c > 0$ . Now, we can rewrite (19) as:

$$\begin{aligned} & \underset{\{\mathbf{w}_k^p, \mathbf{w}_k^c, \gamma_k^p, \gamma_k^c | \forall k \in \mathcal{K}\}}{\text{maximize}} && \sum_{k=1}^K \alpha_k B (\log_2(1 + \gamma_k^p) + \log_2(1 + \gamma_k^c)) \\ & \text{subject to} && (7) \end{aligned} \quad (21a)$$

$$\Gamma_k^p \geq \gamma_k^p \quad \forall k \in \mathcal{K} \quad (21b)$$

$$\Gamma_{i,k}^c \geq \gamma_k^c \quad \forall i \in \mathcal{M}_k \text{ and } \forall k \in \mathcal{K} \quad (21c)$$

$$\begin{aligned} & \sum_{k \in \mathcal{K}} B \left( f_\theta \left( \|\mathbf{w}_{n,k}^p\|_2^2 \right) \log_2(1 + \gamma_k^p) + \right. \\ & \left. f_\theta \left( \|\mathbf{w}_{n,k}^c\|_2^2 \right) \log_2(1 + \gamma_k^c) \right) \leq C_n \quad \forall n \in \mathcal{N}. \end{aligned} \quad (21d)$$

Problem (21) is still non-convex despite relaxing the binary constraints. This is because the feasible set defined by constraints (21b)-(21d) is a non-convex set. To overcome this challenge, we use some algebraic manipulations to rewrite the problem (21) in a form that is easier to tackle, as described next in the text.

### B. Clustering

Given the SINR expressions in (15) and (16), we can equivalently write the constraints (21b) and (21c) as:

$$\sum_{j \in \mathcal{K} \setminus k} |\mathbf{h}_k^H \mathbf{w}_j^p|^2 + \sum_{l \in \mathcal{K} \setminus \Phi_k} |\mathbf{h}_k^H \mathbf{w}_l^c|^2 + \sigma^2 - \frac{|\mathbf{h}_k^H \mathbf{w}_k^p|^2}{\gamma_k^p} \leq 0 \quad (22)$$

$$T_k + \sum_{l \in \mathcal{K} \setminus \Phi_k} |\mathbf{h}_k^H \mathbf{w}_l^c|^2 + \sum_{\substack{m \in \Phi_k \\ \pi_k(m) > \pi_k(i)}} |\mathbf{h}_k^H \mathbf{w}_m^c|^2 - \frac{|\mathbf{h}_k^H \mathbf{w}_k^c|^2}{\gamma_k^c} \leq 0 \quad (23)$$

Note that the function  $\frac{|\mathbf{h}_k^H \mathbf{w}_k^p|^2}{\gamma_k^p}$  in (22) is of the form  $\frac{\|x\|_2^2}{\beta}$ , which is a convex quadratic function [38]–[40]. This reformulation is useful, because it converts the constraints (21b) and (21c) to a difference of convex functions, which facilitates the inner-convex approximation. Let  $\mathbf{t}_k = [t_{1,k}^p, t_{1,k}^c, \dots, t_{N,k}^p, t_{N,k}^c]^T$  and  $\mathbf{d}_k = [d_k^p, d_k^c]$  be slack variables. With the help of such new variables  $\mathbf{t}_k$  and  $\mathbf{d}_k$ , we can rewrite the optimization problem (21) by splitting the constraint in (21d) into five simpler constraints as follows:

$$\begin{aligned} & \underset{\{\mathbf{w}_k^p, \mathbf{w}_k^c, \gamma_k, \mathbf{d}_k, \mathbf{t}_k | \forall k \in \mathcal{K}\}}{\text{maximize}} \quad \sum_{k=1}^K g_1(\gamma_k^p, \gamma_k^c) \end{aligned} \quad (24a)$$

$$\text{subject to} \quad (7), (22) - (23) \quad (24b)$$

$$\sum_{k \in \mathcal{K}} (t_{n,k}^p d_k^p + t_{n,k}^c d_k^c) \leq C_n/B \quad \forall n \in \mathcal{N} \quad (24c)$$

$$f_\theta(\|\mathbf{w}_{n,k}^p\|_2^2) \leq t_{n,k}^p \text{ and } f_\theta(\|\mathbf{w}_{n,k}^c\|_2^2) \leq t_{n,k}^c \quad (24d)$$

$$\log_2(1 + \gamma_k^p) \leq d_k^p \quad (24e)$$

$$\log_2(1 + \gamma_k^c) \leq d_k^c \quad \forall n \in \mathcal{N} \text{ and } \forall k \in \mathcal{K} \quad (24f)$$

where the function  $g_1(\gamma_k^p, \gamma_k^c)$  is defined as:  $g_1(\gamma_k^p, \gamma_k^c) = \alpha_k B (\log_2(1 + \gamma_k^p) + \log_2(1 + \gamma_k^c))$ . The following proposition illustrates how problems (21) and (24) are indeed equivalent to each other. Let  $\mathbf{t}, \mathbf{d}$  be slack variables defined as:  $\mathbf{t} \triangleq [\mathbf{t}_1^T, \dots, \mathbf{t}_K^T]^T$  and  $\mathbf{d} \triangleq [\mathbf{d}_1^T, \dots, \mathbf{d}_K^T]^T$

*Proposition 1.*  $(\mathbf{w}^*, \gamma^*)$  is a stationary solution of (21) if and only if there exist  $(\mathbf{t}^*, \mathbf{d}^*)$  such that  $(\mathbf{w}^*, \gamma^*, \mathbf{t}^*, \mathbf{d}^*)$  is a stationary solution of (24).

*Proof.* The respective formulations of problems (21) and (24) share the same objective function. Moreover, the maximum transmit power constraint (7) is the same in both problems. Constraints



in (22)-(23) are equivalent mathematical manipulations of constraints (21b)-(21c). Furthermore, constraint (21d) is equivalent to constraints (24c)–(24f), after introducing the slack variables  $\mathbf{t}, \mathbf{d}$ . Therefore, optimization problems (21) and (24) are equivalent to each other.  $\square$

Solving problem (24) helps finding the clusters which serve the private and common messages respectively for each user. But since (24) is a non-convex problem, we propose using ICA, so as to approximate the non-convex feasible set of problem (24) as described next.

### C. Inner Convex Approximations (ICA)

Although problem (24) is a non-convex problem, this paper adopts well-chosen ICA techniques to convexify its feasibility set, which is defined by constraints in (24b)–(24f). We start with some algebraic transformations to constraint (24c). We note that the bilinear function  $t_{n,k}^p d_k^p + t_{n,k}^c d_k^c$  can be equivalently written as

$$t_{n,k}^p d_k^p + t_{n,k}^c d_k^c = \frac{1}{2} \sum_{o \in \{p,c\}} [(t_{n,k}^o + d_k^o)^2 - (t_{n,k}^o)^2 - (d_k^o)^2] \quad (25)$$

This form is equivalent to a convex plus concave functions (difference of two convex functions). We proceed by introducing a convex upper bound to the bilinear function in (25), by keeping the convex part and replacing the concave function with its first-order approximation.

Let  $\tilde{g}_{2n}(\mathbf{t}, \mathbf{d}, \tilde{\mathbf{t}}, \tilde{\mathbf{d}})$  be defined as:

$$\begin{aligned} \tilde{g}_{2n}(\mathbf{t}, \mathbf{d}, \tilde{\mathbf{t}}, \tilde{\mathbf{d}}) \triangleq & \sum_{k \in \mathcal{K}} \sum_{o \in \{p,c\}} \left( \frac{1}{2} (t_{n,k}^o + d_k^o)^2 - \frac{1}{2} (\tilde{t}_{n,k}^o)^2 - \frac{1}{2} (\tilde{d}_k^o)^2 \right. \\ & \left. - \tilde{t}_{n,k}^o (t_{n,k}^o - \tilde{t}_{n,k}^o) - \tilde{d}_k^o (d_k^o - \tilde{d}_k^o) \right) - C_n/B \quad \forall n \in \mathcal{N} \end{aligned} \quad (26)$$

where  $(\tilde{\mathbf{t}}, \tilde{\mathbf{d}})$  are feasible fixed values, which satisfy constraints (24c)–(24f).

*Proposition 2.* For any feasible vectors  $(\tilde{\mathbf{t}}, \tilde{\mathbf{d}})$ , the function  $\tilde{g}_{2n}(\mathbf{t}, \mathbf{d}, \tilde{\mathbf{t}}, \tilde{\mathbf{d}})$  satisfies:

$$\tilde{g}_{2n}(\mathbf{t}, \mathbf{d}, \tilde{\mathbf{t}}, \tilde{\mathbf{d}}) \geq \underbrace{\sum_{k \in \mathcal{K}} (t_{n,k}^p d_k^p + t_{n,k}^c d_k^c)}_{g_{2n}(\mathbf{t}, \mathbf{d})} - C_n/B \quad (27)$$

for all feasible values  $(\tilde{\mathbf{t}}, \tilde{\mathbf{d}})$  and all  $n \in \mathcal{N}$ .

*Proof.* We note that the function

$$g_{n,k}(\mathbf{y}) \triangleq \frac{1}{2} \sum_{o \in \{p,c\}} \left[ \underbrace{(t_{n,k}^o + d_k^o)^2}_{g_{n,k,o}^+(\mathbf{y})} - \underbrace{((t_{n,k}^o)^2 + (d_k^o)^2)}_{g_{n,k,o}^-(\mathbf{y})} \right] \quad (28)$$

has a structure of difference of two convex functions, where both functions  $g_{n,k,o}^+(\mathbf{y})$  and  $g_{n,k,o}^-(\mathbf{y})$  are convex, and  $\mathbf{y} = [\mathbf{t}^T, \mathbf{d}^T]^T$ . By keeping the convex part  $g_{n,k,o}^+(\cdot)$  unchanged and linearising the concave part  $-g_{n,k,o}^-(\cdot)$  using the first order approximation around the point  $(\tilde{t}_{n,k}^o, \tilde{d}_k^o) \forall o \in \{p, c\}$ , we get the following convex upper approximation of the function  $g_{n,k}(\mathbf{y})$ :

$$\tilde{g}_{n,k}(\mathbf{y}, \tilde{\mathbf{y}}) \triangleq \frac{1}{2} \sum_{o \in \{p,c\}} g_{n,k,o}^+(\mathbf{y}) - g_{n,k,o}^-(\tilde{\mathbf{y}}) - \nabla_{\mathbf{y}} g_{n,k,o}^-(\tilde{\mathbf{y}})^T (\mathbf{y} - \tilde{\mathbf{y}}), \quad (29)$$

where  $\tilde{\mathbf{y}} = [\tilde{\mathbf{t}}^T, \tilde{\mathbf{d}}^T]^T$ .

We can write the function  $\tilde{g}_{n,k}(\mathbf{y}, \tilde{\mathbf{y}})$  as

$$\begin{aligned} \tilde{g}_{n,k}(\mathbf{y}, \tilde{\mathbf{y}}) =: & \sum_{o \in \{p,c\}} \left( \frac{1}{2} (t_{n,k}^o + d_k^o)^2 - \frac{1}{2} (\tilde{t}_{n,k}^o)^2 - \frac{1}{2} (\tilde{d}_k^o)^2 \right. \\ & \left. - \tilde{t}_{n,k}^o (t_{n,k}^o - \tilde{t}_{n,k}^o) - \tilde{d}_k^o (d_k^o - \tilde{d}_k^o) \right) \end{aligned} \quad (30)$$

Based on the convexity of  $g_{n,k}^-(\mathbf{y})$ , the following inequality follows:  $t_{n,k}^p d_k^p + t_{n,k}^c d_k^c = g_{n,k}(\mathbf{y}) \leq \tilde{g}_{n,k}(\mathbf{y}, \tilde{\mathbf{y}})$ . This completes the proof of proposition 2.  $\square$

Afterwards, we perform distinct ICA operations for the remaining constraints. More precisely, for constraint (24d), we linearize the concave functions  $f_\theta \left( \|\mathbf{w}_{n,k}^p\|_2^2 \right)$  and  $f_\theta \left( \|\mathbf{w}_{n,k}^c\|_2^2 \right)$  around  $\tilde{\mathbf{w}}_{n,k}^p$  and  $\tilde{\mathbf{w}}_{n,k}^c$ , respectively. This leads to the following inner-convex approximation of the set defined by the constraints in (24d):

$$\tilde{g}_3(\mathbf{w}_{n,k}^p, \tilde{\mathbf{w}}_{n,k}^p) \triangleq f_\theta \left( \|\mathbf{w}_{n,k}^p\|_2^2 \right) + \nabla f_\theta \left( \|\mathbf{w}_{n,k}^p\|_2^2 \right) \left( \|\mathbf{w}_{n,k}^p\|_2^2 - \|\tilde{\mathbf{w}}_{n,k}^p\|_2^2 \right) \quad (31)$$

$$\tilde{g}_4(\mathbf{w}_{n,k}^c, \tilde{\mathbf{w}}_{n,k}^c) \triangleq f_\theta \left( \|\mathbf{w}_{n,k}^c\|_2^2 \right) + \nabla f_\theta \left( \|\mathbf{w}_{n,k}^c\|_2^2 \right) \left( \|\mathbf{w}_{n,k}^c\|_2^2 - \|\tilde{\mathbf{w}}_{n,k}^c\|_2^2 \right) \quad (32)$$

We follow the same procedure with constraints (24e) and (24f), where we linearize the concave functions  $\log_2(1 + \gamma_k^p)$ ,  $\log_2(1 + \gamma_k^c)$  around  $\tilde{\gamma}_k^p$  and  $\tilde{\gamma}_k^c$ , respectively. We obtain the following equations which define an inner-convex approximation of the non-convex feasible set defined by

constraints (24e) and (24f):

$$\tilde{g}_5(\gamma_k^p, \tilde{\gamma}_k^p) \triangleq \log_2(1 + \tilde{\gamma}_k^p) + \frac{1}{(1 + \tilde{\gamma}_k^p) \ln(2)} (\gamma_k^p - \tilde{\gamma}_k^p) \leq 0 \quad (33)$$

$$\tilde{g}_6(\gamma_k^c, \tilde{\gamma}_k^c) \triangleq \log_2(1 + \tilde{\gamma}_k^c) + \frac{1}{(1 + \tilde{\gamma}_k^c) \ln(2)} (\gamma_k^c - \tilde{\gamma}_k^c) \leq 0 \quad (34)$$

Concerning the SINR constraints in (22) and (23), we note that if  $(\tilde{\mathbf{w}}, \tilde{\gamma})$  is a feasible point of (24), then the following holds:

$$\frac{|\mathbf{h}_k^H \mathbf{w}_k^p|^2}{\gamma_k^p} \geq \frac{2\Re\left\{(\tilde{\mathbf{w}}_k^p)^H \mathbf{h}_k \mathbf{h}_k^H \mathbf{w}_k^p\right\}}{\tilde{\gamma}_k^p} - \frac{|\mathbf{h}_k^H \tilde{\mathbf{w}}_k^p|^2}{(\tilde{\gamma}_k^p)^2} \gamma_k^p \quad (35)$$

and

$$\frac{|\mathbf{h}_i^H \mathbf{w}_k^c|^2}{\gamma_k^c} \geq \frac{2\Re\left\{(\tilde{\mathbf{w}}_k^c)^H \mathbf{h}_i \mathbf{h}_i^H \mathbf{w}_k^c\right\}}{\tilde{\gamma}_k^c} - \frac{|\mathbf{h}_i^H \tilde{\mathbf{w}}_k^c|^2}{(\tilde{\gamma}_k^c)^2} \gamma_k^c \quad (36)$$

where  $\Re\{\cdot\}$  is the real part of a complex number. Based on inequalities (35) and (36), we can establish inner-convex approximations of the constraints in (22) and (23) as follows:

$$\begin{aligned} \tilde{g}_7(\mathbf{w}, \gamma_k^p; \tilde{\mathbf{w}}, \tilde{\gamma}_k^p) &\triangleq \sum_{j \in \mathcal{K} \setminus k} |\mathbf{h}_k^H \mathbf{w}_j^p|^2 + \sum_{l \in \mathcal{K} \setminus \Phi_k} |\mathbf{h}_k^H \mathbf{w}_l^p|^2 + \sigma^2 \\ &\quad - \frac{2\Re\left\{(\tilde{\mathbf{w}}_k^p)^H \mathbf{h}_k \mathbf{h}_k^H \mathbf{w}_k^p\right\}}{\tilde{\gamma}_k^p} + \frac{|\mathbf{h}_k^H \tilde{\mathbf{w}}_k^p|^2}{(\tilde{\gamma}_k^p)^2} \gamma_k^p \end{aligned} \quad (37)$$

$$\begin{aligned} \tilde{g}_8(\mathbf{w}, \gamma_k^c; \tilde{\mathbf{w}}, \tilde{\gamma}_k^c) &\triangleq T_k + \sum_{l \in \mathcal{K} \setminus \Phi_k} |\mathbf{h}_k^H \mathbf{w}_l^c|^2 \\ &\quad + \sum_{\substack{m \in \Phi_k \\ \pi_k(m) > \pi_k(i)}} |\mathbf{h}_k^H \mathbf{w}_m^c|^2 + \frac{|\mathbf{h}_i^H \tilde{\mathbf{w}}_k^c|^2}{(\tilde{\gamma}_k^c)^2} \gamma_k^c \\ &\quad - \frac{2\Re\left\{(\tilde{\mathbf{w}}_k^c)^H \mathbf{h}_i \mathbf{h}_i^H \mathbf{w}_k^c\right\}}{\tilde{\gamma}_k^c} \end{aligned} \quad (38)$$

The next subsection presents the strongly inner-convex approximations of problem (21), and describes the algorithm that solves it.

#### D. Strongly ICA based Algorithm

The functions in (26), (31)–(34) and (37)–(38) define a convex feasible set, which represents an inner-approximation of the non-convex feasible set of problem (24). The idea of our approach

is to iteratively solve the optimization problem defined with this approximation. After each iteration, we refine the ICA of the feasible set in (24), and keep iterating until convergence to a stationary solution, as described next. The approximate optimization problem is defined as follows:

$$\begin{aligned} & \underset{\{\mathbf{w}_k^p, \mathbf{w}_k^c, \gamma_k, \mathbf{d}_k, \mathbf{t}_k | \forall k \in \mathcal{K}\}}{\text{maximize}} && \sum_{k=1}^K g_1(\gamma_k^p, \gamma_k^c) - g_9(\mathbf{w}, \gamma; \tilde{\mathbf{w}}, \tilde{\gamma}) \end{aligned} \quad (39a)$$

$$\text{subject to} \quad (7) \quad (39b)$$

$$\tilde{g}_{2n}(\mathbf{t}, \mathbf{d}, \tilde{\mathbf{t}}, \tilde{\mathbf{d}}) \leq 0 \quad (39c)$$

$$\tilde{g}_3(\mathbf{w}_{n,k}^p, \tilde{\mathbf{w}}_{n,k}^p) \leq 0 \quad (39d)$$

$$\tilde{g}_4(\mathbf{w}_{n,k}^c, \tilde{\mathbf{w}}_{n,k}^c) \leq 0 \quad (39e)$$

$$\tilde{g}_5(\gamma_k^p, \tilde{\gamma}_k^p) \leq 0 \quad (39f)$$

$$\tilde{g}_6(\gamma_k^c, \tilde{\gamma}_k^c) \leq 0 \quad (39g)$$

$$\tilde{g}_7(\mathbf{w}, \gamma_k^p; \tilde{\mathbf{w}}, \tilde{\gamma}_k^p) \leq 0 \quad (39h)$$

$$\tilde{g}_8(\mathbf{w}, \gamma_k^c; \tilde{\mathbf{w}}, \tilde{\gamma}_k^c) \leq 0 \quad (39i)$$

Here,  $g_9(\mathbf{w}, \gamma; \tilde{\mathbf{w}}, \tilde{\gamma})$  is a proximal term to assure that the objective is a strongly concave function, and is defined as follows:

$$g_9(\mathbf{w}, \gamma; \tilde{\mathbf{w}}, \tilde{\gamma}) = \rho_1 \|\mathbf{w} - \tilde{\mathbf{w}}\|_2^2 + \rho_2 \|\gamma - \tilde{\gamma}\|_2^2. \quad (40)$$

Let  $\mathbf{Z} = [\mathbf{w}^T, \gamma^T, \mathbf{t}^T, \mathbf{d}^T]^T$  be a vector stacking all the optimization variables of the problem (39). Let  $\hat{\mathbf{Z}}_v$  be the variables computed at iteration  $v$  as the optimal solution of problem (39), and let  $\tilde{\mathbf{Z}} = [\tilde{\mathbf{w}}^T, \tilde{\gamma}^T, \tilde{\mathbf{t}}^T, \tilde{\mathbf{d}}^T]^T$  be the point at which we compute the approximate solution of problem (39) at iteration  $v$ . Furthermore, let  $\mathcal{Z}$  denote the convex feasible set of problem (39) defined by constraints (39b)–(39i). The algorithm starts by initializing the vector  $\tilde{\mathbf{Z}}$ , around which we compute the next iteration. The initialization process starts by computing feasible MRC beamformers for the users' messages when considering TIN scheme, and for both private and common messages when considering RS-CMD scheme. Based on this initialization, we compute the vector  $\tilde{\gamma}$  using equations (15) and (16). Note that the sets  $\{\Phi_k\}_{k=1}^K$  are computed using Algorithm 1. The initialization of vectors  $\tilde{\mathbf{t}}, \tilde{\mathbf{d}}$  is done solving (24d)–(24f) by replacing inequalities with equalities. After solving the problem (39) at iteration  $v$ , we get the optimal

values stacked in vector  $\widehat{\mathbf{Z}}_v$ . Using  $\widehat{\mathbf{Z}}_v$ , we compute the vector  $\tilde{\mathbf{Z}}$  for the next iteration. The detailed steps of the iterative algorithm to solve problem (21) are summarized in Algorithm 2 description below. The following theorem proves that Algorithm 2 produces a stationary solution

---

**Algorithm 2** Inner convex approximation of (21).

---

- 1: **Initialize:**  $v \leftarrow 0$ ,  $\tilde{\mathbf{Z}} \in \mathcal{Z}$ ,  $\rho_1 > 0$ ,  $\rho_2 > 0$ ,  $\xi \ll 1$ ,  $\xi \in \mathbb{R}_+$  and  $\theta = \theta_v$ .
  - 2: **while**  $\widehat{\mathbf{Z}}_v$  not a stationary solution of (21) **do**
  - 3:     Solve the convex problem (39) and compute  $\widehat{\mathbf{Z}}_v$
  - 4:      $\tilde{\mathbf{Z}} \leftarrow \tilde{\mathbf{Z}} + \beta_v (\widehat{\mathbf{Z}}_v - \tilde{\mathbf{Z}})$  for some  $\beta_v \in (0, 1]$
  - 5:     **if**  $\theta_v \geq \xi$  **then**  $\theta_v = \delta \theta_v$  and  $\delta \in (0, 1)$
  - 6:     **end if**
  - 7:      $v \leftarrow v + 1$
  - 8: **end while**
- 

of problem (21).

*Theorem 1.* Let  $\rho_1, \rho_2 > 0$ , and let the step size sequence  $\{\beta_v\}$  satisfy  $\beta_v \in (0, 1]$ ,  $\beta_v \rightarrow 0$ , and  $\sum_v \beta_v = +\infty$ . Then  $\{\widehat{\mathbf{Z}}_v\}$ , the sequence generated by Algorithm 2, is bounded, and converges to  $\{\widehat{\mathbf{Z}}_v^*\}$ , which is a stationary solution of problem (39), such that  $(\gamma^*, \mathbf{t}^*, \mathbf{d}^*) > 0$ . Therefore, (according to proposition 1),  $(\mathbf{w}^*, \gamma^*)$  is also a stationary point of problem (21).

*Proof.* The steps of the proof rely on showing that the objective and constraints of problem (39) satisfy the conditions of [41, Sec. II], which would guarantee the convergence to a stationary point as illustrated in [41, Theorem 2]. Towards this end, we show next that the function  $\tilde{g}_{2n}(\mathbf{t}, \mathbf{d}; \tilde{\mathbf{t}}, \tilde{\mathbf{d}})$  satisfies the following properties:

- C1)  $\tilde{g}_{2n}(\tilde{\mathbf{y}}, \tilde{\mathbf{y}}) = g_{2n}(\tilde{\mathbf{y}})$
- C2)  $\tilde{g}_{2n}(\mathbf{y}, \tilde{\mathbf{y}}) \geq g_{2n}(\mathbf{y})$ ,  $\forall \tilde{\mathbf{y}} \in \mathcal{Z}$
- C3)  $\tilde{g}_{2n}(\bullet, \tilde{\mathbf{y}})$  is a convex function,  $\forall \tilde{\mathbf{y}} \in \mathcal{Z}$
- C4)  $\tilde{g}_{2n}(\bullet, \bullet)$  is a continuous function on the feasible set.
- C5)  $\nabla_{\mathbf{y}} \tilde{g}_{2n}(\tilde{\mathbf{y}}, \tilde{\mathbf{y}}) = \nabla_{\mathbf{y}} g_{2n}(\tilde{\mathbf{y}})$
- C6) The function  $\nabla_{\mathbf{y}} \tilde{g}_{2n}(\bullet, \bullet)$  is continuous on the feasible set

C1 is verified by substituting  $\mathbf{y} = [\mathbf{t}^T, \mathbf{d}^T]^T$  in (26) by  $\tilde{\mathbf{y}} = [\tilde{\mathbf{t}}^T, \tilde{\mathbf{d}}^T]^T$ . Comparing the result with  $g_{2n}(\tilde{\mathbf{y}})$  then yields the equality. C2 follows directly from proposition 2. C3 also holds, since the function  $\tilde{g}_{2n}(\bullet, \tilde{\mathbf{y}})$  with fixed  $\tilde{\mathbf{y}}$  consists of a convex quadratic function plus a linear function, which is convex. Further, the function  $\tilde{g}_{2n}(\bullet, \bullet)$  is a difference of two convex functions, and so

C4 is also true. Finally, to prove C5 and C6, take the partial derivative of the function  $g_{2n}(\bullet, \tilde{\mathbf{y}})$  as follows:

$$\nabla_{\mathbf{y}} \tilde{g}_{2n}(\mathbf{y}, \tilde{\mathbf{y}}) = \begin{cases} \frac{\partial \tilde{g}_{2n}(\bullet, \tilde{\mathbf{y}})}{\partial t_{n,k}} & \triangleq \sum_{k \in \mathcal{K}} \sum_{o \in \{p,c\}} ((t_{n,k}^o + d_k^o) - \tilde{t}_{n,k}^o) \quad \forall n \\ \frac{\partial \tilde{g}_{2n}(\bullet, \tilde{\mathbf{y}})}{\partial d_k} & \triangleq \sum_{k \in \mathcal{K}} \sum_{o \in \{p,c\}} ((t_{n,k}^o + d_k^o) - \tilde{d}_k^o) \end{cases} \quad (41)$$

Similarly, the partial derivative of  $g_{2n}(\mathbf{y})$  is:

$$\nabla_{\mathbf{y}} g_{2n}(\mathbf{y}) = \begin{cases} \frac{\partial g_{2n}(\mathbf{y})}{\partial t_{n,k}} & \triangleq \sum_{k \in \mathcal{K}} (d_k^p + d_k^c) \\ \frac{\partial g_{2n}(\mathbf{y})}{\partial d_k} & \triangleq \sum_{k \in \mathcal{K}} (t_{n,k}^p + t_{n,k}^c) \end{cases} \quad (42)$$

C5 then follows by substituting  $\mathbf{y}$  with  $\tilde{\mathbf{y}}$  in both (41) and (42). C6 also holds since that the function  $\nabla_{\mathbf{y}} \tilde{g}_{2n}(\bullet, \bullet)$  is bilinear. The above proof verifies that the function  $\tilde{g}_{2n}(\mathbf{t}, \mathbf{d}; \tilde{\mathbf{t}}, \tilde{\mathbf{d}})$  satisfies the properties C1-C6. One can similarly check that all other functions associated with the optimization problem (39) also satisfy C1-C6, which completes the proof.  $\square$

After solving problem (24), we can determine the clusters for private and common messages as follows:

$$\mathcal{K}_n^p = \left\{ k \mid \|\mathbf{w}_{n,k}^p\|_2^2 \geq \epsilon_1 \right\}, \quad (43)$$

$$\mathcal{K}_n^c = \left\{ k \mid \|\mathbf{w}_{n,k}^c\|_2^2 \geq \epsilon_2 \right\}, \quad (44)$$

Where  $\epsilon_1$  and  $\epsilon_2$  are positive constants, which are set in the simulations section to -80 dBm/Hz.

### E. Beamforming and RS mode Selection

After fixing the clusters  $\mathcal{K}_n^p$  and  $\mathcal{K}_n^c$  as described above, the paper now focuses on determining the beamforming vectors by revisiting problem (39). Note that when the clusters are fixed, the optimization variables become the group sparse beamforming vectors  $\{\mathbf{w}_k^p, \mathbf{w}_k^c, \gamma_k \mid \forall k \in \mathcal{K}\}$ .

Mathematically, the optimization problem (39) for fixed clusters can be written as:

$$\begin{aligned} & \underset{\{\mathbf{w}_k^p, \mathbf{w}_k^c, \gamma_k | \forall k \in \mathcal{K}\}}{\text{maximize}} && \sum_{k=1}^K g_1(\gamma_k^p, \gamma_k^c) - g_9(\mathbf{w}, \gamma; \tilde{\mathbf{w}}, \tilde{\gamma}) \end{aligned} \quad (45a)$$

$$\text{subject to} \quad g_{10}(\gamma_k^p, \tilde{\gamma}_k^p, \gamma_k^c, \tilde{\gamma}_k^c) \leq 0 \quad (45b)$$

$$\sum_{k \in \mathcal{K}_n^p} \|\mathbf{w}_{n,k}^p\|_2^2 + \sum_{k \in \mathcal{K}_n^c} \|\mathbf{w}_{n,k}^c\|_2^2 \leq P_n^{\text{Max}} \quad \forall n \in \mathcal{N} \quad (45c)$$

$$g_7(\mathbf{w}, \gamma_k^p; \tilde{\mathbf{w}}, \tilde{\gamma}_k^p) \leq 0 \quad (45d)$$

$$g_8(\mathbf{w}, \gamma_k^c; \tilde{\mathbf{w}}, \tilde{\gamma}_k^c) \leq 0 \quad (45e)$$

where  $g_{10}(\gamma_k^p, \tilde{\gamma}_k^p, \gamma_k^c, \tilde{\gamma}_k^c) \leq 0$  represents the backhaul constraint, and where the function  $g_{10}(\cdot)$  is defined as:

$$\begin{aligned} g_{10}(\gamma_k^p, \tilde{\gamma}_k^p, \gamma_k^c, \tilde{\gamma}_k^c) &\triangleq \sum_{k \in \mathcal{K}_n^p} g_5(\gamma_k^p, \tilde{\gamma}_k^p) \\ &+ \sum_{k \in \mathcal{K}_n^c} g_6(\gamma_k^c, \tilde{\gamma}_k^c) - C_n/B. \end{aligned} \quad (46)$$

We note that problem (45) is similar to problem (39); however, the association variables are fixed here and the goal is to find beamforming vectors with good quality. Toward this goal, we suggest using Algorithm 3 shown below to obtain a stationary solution  $(\mathbf{w}^*, \gamma^*)$  to the beamforming problem with fixed clusters. Here,  $\mathbf{Y} = [\mathbf{w}^T, \gamma^T]^T$ ,  $\tilde{\mathbf{Y}} = [\tilde{\mathbf{w}}^T, \tilde{\gamma}^T]^T$  and  $\mathcal{Y}$  is the feasible set of problem (45).

---

**Algorithm 3** Inner convex approximation of beamforming problem with fixed clusters.

---

- 1: Initialize:  $v \leftarrow 0$ ,  $\tilde{\mathbf{Y}} \in \mathcal{Y}$  and  $\rho_1 > 0, \rho_2 > 0$
  - 2: **while**  $\hat{\mathbf{Y}}_v$  not a stationary solution. **do**
  - 3:     Solve the convex problem (45) and compute  $\hat{\mathbf{Y}}_v$
  - 4:      $\tilde{\mathbf{Y}} \leftarrow \tilde{\mathbf{Y}} + \beta_v (\hat{\mathbf{Y}}_v - \tilde{\mathbf{Y}})$  for some  $\beta_v \in (0, 1]$
  - 5:      $v \leftarrow v + 1$
  - 6: **end while**
- 

## F. Complexity Analysis

The overall approach of joint clustering, RS mode and beamforming vectors design is split into two stages. In the first one we use Algorithm 2 to find the clusters of BSs which serve the

private message and common message of each user respectively. After that, we use the Algorithm 3 to find a high-quality solution of beamforming vectors and RS which are also feasible to the original problem (21). In the following, we describe the overall complexity of such an approach.

At each iteration of Algorithm 2, which is used to determine the clusters, we need to solve a convex problem, precisely problem (39), which has a logarithm plus a proximal term as an objective function. The logarithmic part can be linearised as in equation (33), which gives a quadratic convex problem which can be easily cast as a second order cone program (SOCP); see [42] and references therein. SOCP problems can be solved using interior-point methods with a complexity of  $\mathcal{O}(NKL)^{3.5}$  via general-purpose solvers, e.g. SDPT3 or MOSEK. After clustering, the beamforming vectors and the RS mode are determined using Algorithm 3, which can similarly cast as an SOCP using a similar argument as above. Let  $V_{\max}$  be the worst-case fixed number of iterations needed for the Algorithm 2 (or Algorithm 3) to converge. The overall computational complexity to implement Algorithm 2 and Algorithm 3 becomes, therefore,  $2V_{\max}(NKL)^{3.5}$ . Note this is a rather an upper bound on the complexity metric, since solving the sparse optimization problem (45) is typically much faster than solving problem (39), and so it needs a smaller number of iterations for convergence.

## V. NUMERICAL RESULTS

In this section, we present an extensive set of numerical simulations to demonstrate the performance of our proposed approach. The system setup considers a C-RAN consisting of a 7-cell wrapped-around network. In each cell, there exists a BS at the center, which is connected to the cloud via a limited capacity backhaul link. The simulations results illustrated in this section assume the parameters summarized in table II, unless mentioned otherwise in the text. In particular, for illustration, all BS's share the same backhaul constraint, and all BS's operate at the same nominal maximum transmission power.

In addition to the dynamic clustering algorithms applied for both TIN and RS-CMD, in which we jointly optimize the BSs clusters together with the beamforming vectors, we also consider a static clustering algorithm. Such static clustering, considered herein as a clustering baseline approach, adopts a path-loss information-based approach, and so the beamforming vectors are optimized for fixed (static) clusters. In the following, we explain briefly the static TIN clustering as used in [21], and our extended version of this algorithm to fit the RS-CMD framework.



- **Static TIN:** This scheme is based on clustering procedure described in [21, Algorithm 3]. Once the clusters are fixed, we can solve problem (45) to determine the optimal beamforming vectors.
- **Static RS-CMD:** In this case, we extend the previous procedure to accommodate clusters for private and common messages for each user. Again, when the clusters are fixed, we use Algorithm 3 to solve problem (45) over the private and common beamforming vectors.

Simulation Parameters	
Network Parameter	Value
Channel Bandwidth	10 MHz
Number of Antennas	8
Maximum transmission Power	30 dBm
Antenna gain	15 dBi
Background noise	-169 dBm/Hz
Path-loss	$140.7 + 36.7 \log_{10}(d)$
Log-normal shadowing	8 dB
Rayleigh small scale fading	0 dB

Further, we assume that each user can decode only one additional common message besides its own common message (i.e.,  $D = 1$ ); however, a common message of a user can be decoded by multiple users. Such strategy helps reducing the complexity of the overall algorithm, by limiting the number of successive cancellation stages.

#### A. Impact of Backhaul Capacity

First, we evaluate the performance of RS-CMD scheme in C-RAN, against the state-of-the-art TIN scheme. For both schemes, we consider dynamic and static clustering procedures. In case of dynamic clustering, we use Algorithm 2 and equations (43) and (44) to determine the clusters. Then, we use Algorithm 3 with few iterations, starting from the solution computed at last iteration of Algorithm 2, to compute the beamforming vectors. In the case of fixed static

clusters, we apply Algorithm 3 directly to compute the beamforming vectors for both TIN and RS-CMD.

We first consider a network in which the inter-cell distance between two neighboring BSs is 200m. Fig. 2 shows the achievable sum rate as a function of backhaul capacity when applying these schemes, where we use RS-CMD in both static and dynamic clustering with parameter values  $\mu = 25$  and  $\mu = 60$ . The figure shows that our proposed algorithm, namely RS-CMD with dynamic clustering and  $\mu = 25$ , outperforms the state-of-the art TIN. In fact, compared with static TIN, RS-CMD with  $\mu = 25$  has a significant gain up to 42.3 % at 950 Mbps backhaul capacity.

Fig. 2, particularly, distinguishes between two backhaul capacity regions. In the low backhaul capacity region, the performance is mainly limited by capacity of backhaul links. In this region, due to the scarcity of backhaul resources, a carefully chosen set of users should be assigned to each BS in order to optimize the performance with the available backhaul resources. This explains why the static clustering schemes perform poorly in this region, while the dynamic schemes achieve sum-rates which are close to the capacity upper bound, i.e.,  $7C_n$ . As we move towards higher backhaul capacities, we note that the sum-rate of all schemes increases, especially the proposed approaches which show a significantly higher sum-rate as compared to the state-of-the art schemes under both dynamic and static clustering, i.e., static TIN and dynamic TIN. We further note that as we approach the interference limited region by increasing the backhaul capacity, the effect of RS-CMD becomes more pronounced. This is expected, since our scheme is especially designed to mitigate interference, and so its performance gets better as the interference becomes the limiting factor. Interestingly, the role of dynamic clustering becomes less significant in the interference limited regime. Here, in the 200 meters inter-cell distance, it is likely that a significant number of users have strong channel gains to nearby BSs, which have enough backhaul resources in the interference limited regime. Such observation makes the impact of clustering in this region less significant as compared to RS-CMD. Thus, we observe that RS-CMD with static clustering outperforms dynamic TIN. Finally, in Fig. 2, we observe that RS-CMD scheme with  $\mu = 25$  (referred to as RS-CMD 25) performs better than RS-CMD with  $\mu = 60$ . Such fact is also expected, since increasing  $\mu$  increases the number of users which participate in decoding the common messages of their interferers, which adds more constraints to the optimization problem, and reduces the value of the optimized objective function, as clearly illustrated in Fig. 2. To best illustrate the performance of the proposed algorithm in a larger inter-cell distance, Fig. 3

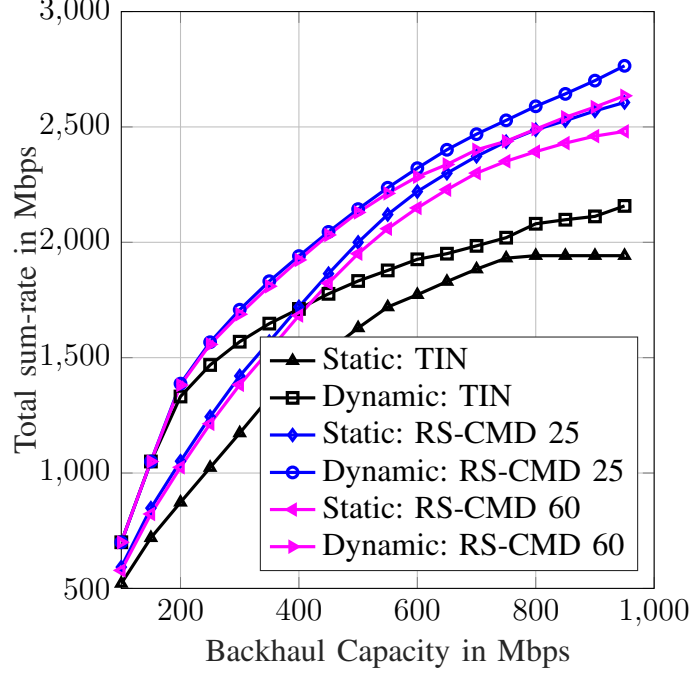


Figure 2: The performance of all studied schemes for a C-RAN with 7 BSs serving 28 users and an inter-cell distance of 200 m

plots the sum-rate across the network versus the backhaul capacity, where the inter-cell distance is set to 400 m. In this case, the cell-edge users are more susceptible to interference from BSs in neighboring cells. On the other hand, the users located near a cell center have better channel gains to BSs in their cell, and weak interference channels to other BSs in other cells. Under such relatively large inter-cell distance, the size of clusters becomes smaller, because only few BSs have strong channel gains to each user as compared to the small inter-cell distance. This explains why Fig. 3 shows that all schemes perform well in the backhaul limited regime. However, as we approach the interference limited regime, the impact of clustering and RS-CMD becomes more significant. In this network, RS-CMD with  $\mu = 25$  achieves a gain up to 61.11 % compared to static TIN, which best highlights the significant gain harvested by common message decoding in C-RAN systems, as illustrated next.

### B. The Role of RS-CMD

To illustrate the impact of common message decoding on the system performance, Fig. 4 plots the sum rates of both the common part and the private part as a function of the backhaul capacity. The figure shows that the rate of the common message increases as the backhaul

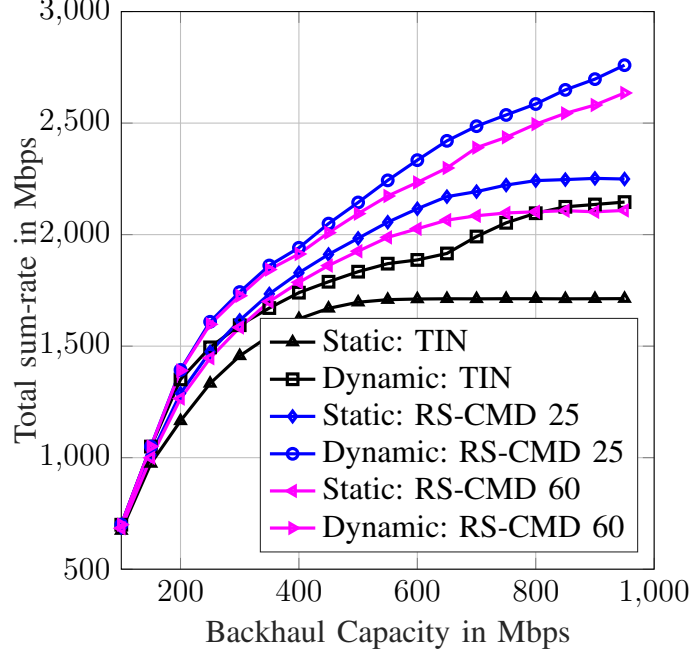


Figure 3: The performance of all studied schemes for a C-RAN with 7 BSs serving 28 users and an inter-cell distance of 400 m

capacity increases, which highlights the impact of RS-CMD in the interference limited regime. Interestingly, as we increase the number of users which decode the common-messages of other users, i.e., as  $\mu$  increases, Fig. 5 shows that the rate of common messages decreases which reduces the total achievable rate, for the same reasons discussed earlier.

### C. Transmission Power Impact on RS-CMD

Fig. 6 shows the sum-rate versus the maximum transmission power, so as to study the impact of transmission power on the performance of RS-CMD. We consider a C-RAN system of 7 BSs serving 28 users. Each BS has 750 Mbps backhaul. The inter-cell distance is set to 200 m. The figure adopts the static clustering for both TIN and RS-CMD, and shows that the gain of RS-CMD compared to TIN increases as the power increases. For  $\mu = 25$ , the gain of RS-CMD over TIN increases from about 12% at 0dBm maximum transmission power, to almost 19% at 40dBm. The rationale for such observation is that as the transmission power increases, the interference experienced in the network increases, and so the role of RS-CMD as an interference mitigation technique becomes more pronounced. In Fig. 6, as the transmission power increases from 0 dBm to 40 dBm we see clearly that the gain of RS-CMD compared to TIN increases. In case of  $\mu = 25$  the gain of RS-CMD over TIN increases from about 12% at 0dBm maximum

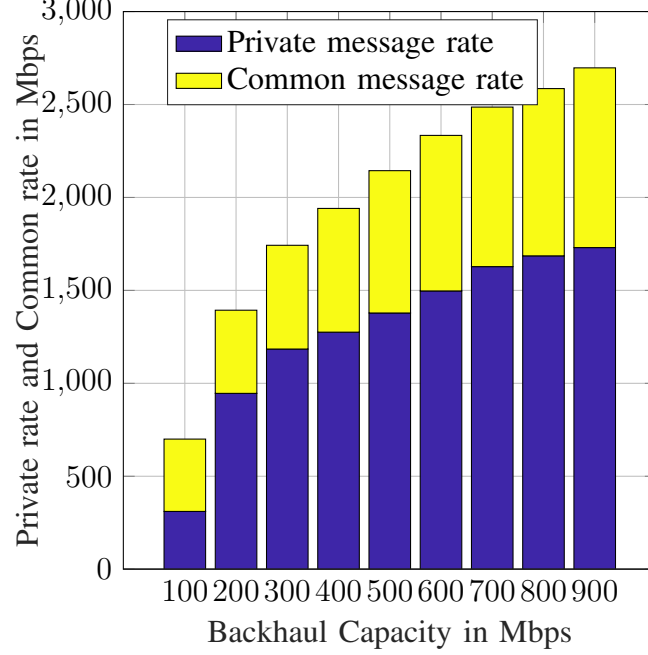


Figure 4: The sum-rate of common message and private message using RS-CMD with  $\mu = 25$  for a C-RAN with 7 BSs serving 28 users and an inter-cell distance of 400 m

transmission power to almost 19% at 40dBm. Intuitively, as the transmission power increases the interference experienced in the network increases as well. Hence, the effectiveness of RS-CMD becomes more pronounced since this method is originally designed to mitigate the interference, while using TIN becomes sub-optimal in high interference regimes.

#### D. Convergence Behavior of Algorithm 2 and Algorithm 3

We now illustrate the convergence behavior of Algorithms 2 and 3, as indicated in Theorem 1. We herein focus on a C-RAN system with 7 BSs serving 28 users and an inter-cell distance of 400 m. All the simulation results are averaged over 80 random realizations. In Fig. 7, we plot the objective function of problem (39) as a function of the number of iterations executed while implementing Algorithm 2, so as to illustrate its convergence. Similarly, Fig. 8 plots the objective function of problem (39) as a function of the number of iterations executed while implementing Algorithm 3, so as to illustrate Algorithm 3 convergence. Both Fig. 7 and Fig. 8 illustrate the fast convergence of both Algorithm 2 and Algorithm 3, respectively, which further highlight the numerical performance of our proposed algorithms. For Algorithm 3 we get the Figure 8.

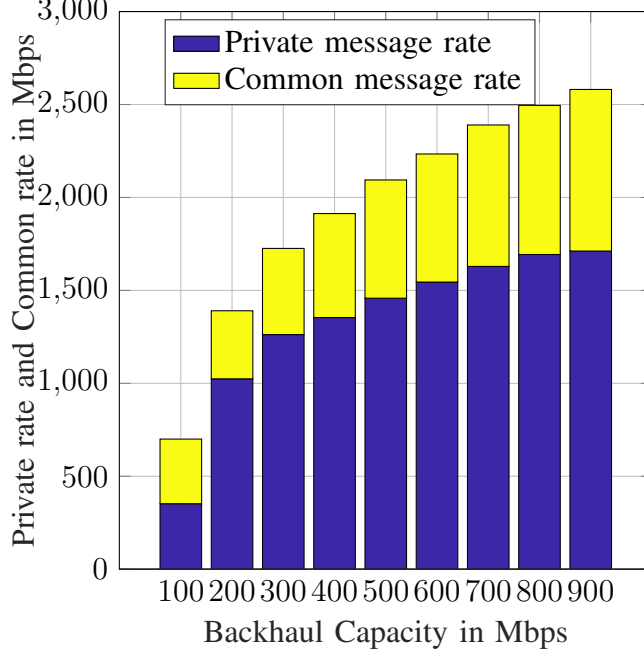


Figure 5: The sum-rate of common message and private message using RS-CMD with  $\mu = 60$  for a C-RAN with 7 BSs serving 28 users and an inter-cell distance of 400 m

#### E. The impact of the Number of Users

Last but not least, we examine the impact of increasing the number of users in the network on the achievable performance. In Fig. 9 we clearly see that dynamic RS-CMD with  $\mu = 25$  outperforms the dynamic TIN. As the number of users increases, the RS-CMD gain improves over TIN. Interestingly, as the number of users approaches the total number of transmit antennas, the gain becomes larger, i.e., when the number of users is 25 in this example. After that, when the number of users exceeds the number of transmit antennas, the achievable sum-rate by dynamic TIN saturates earlier than the dynamic RS-CMD, which further highlights the important role of joint rate splitting and common message decoding in dense networks.

## VI. CONCLUSIONS

This paper amalgamates the benefits of RS in C-RAN for enabling large-scale interference management. We have proposed a transmission scheme for a C-RAN which capitalizes on rate-splitting, common message decoding, beamforming vector design and clustering to mitigate interference and appropriately use the limited backhaul and transmit power resources. For the

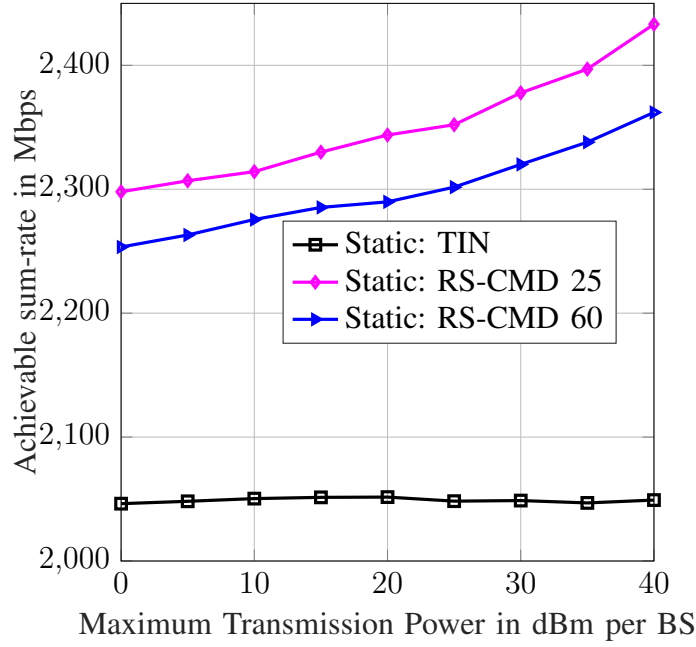


Figure 6: The achievable sum-rate as a function of maximum transmission power, using static TIN and RS-CMD with  $\mu = 25$  for the scenario in which a C-RAN with 7 BSs serving 28 users. Each BS has 750 Mbps backhaul. The inter-cell distance is 200 m

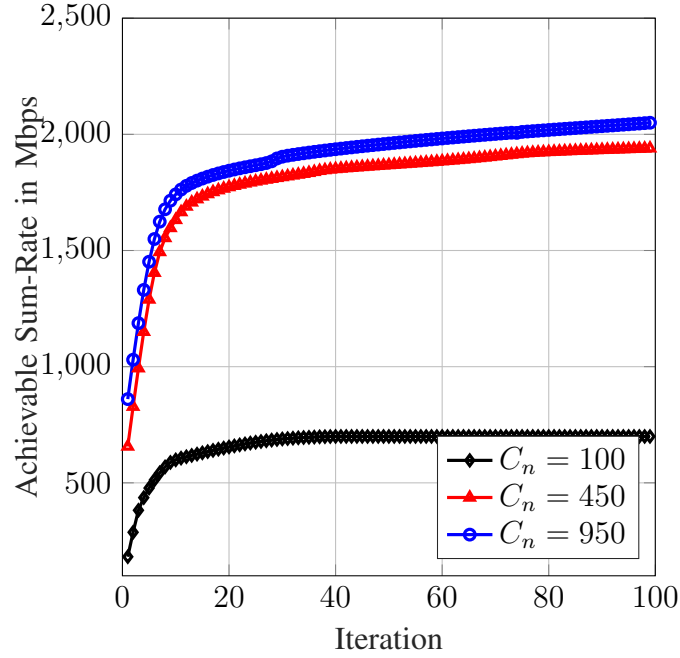


Figure 7: The objective function of (39), using RS-CMD with  $\mu = 25$  for the scenario in which a C-RAN with 7 BSs serving 28 users and an inter-cell distance of 400 m

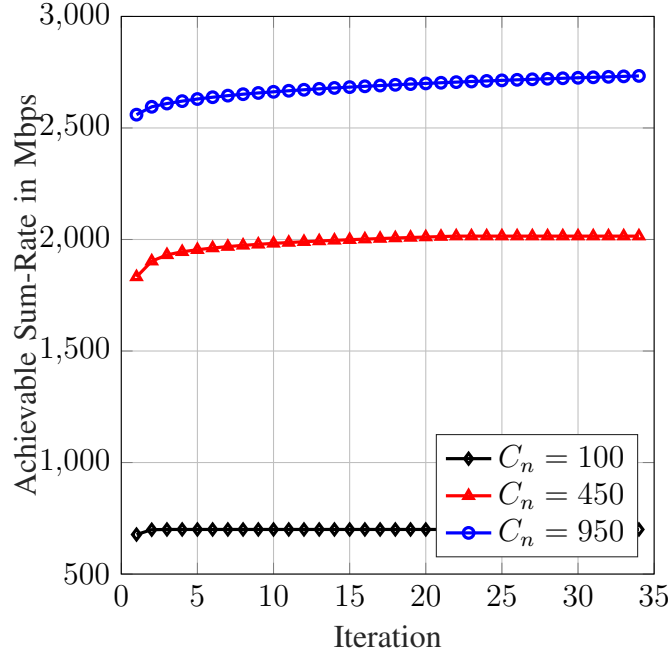


Figure 8: The objective function of (39), using RS-CMD with  $\mu = 25$  for the scenario in which a C-RAN with 7 BSs serving 28 users and an inter-cell distance of 400 m

proposed scheme, we formulated the problem of maximizing the weighted sum-rate subject to finite backhaul capacity and transmit power constraints. We have proposed a solution using  $l_0$  relaxation followed by an ICA framework. Simulations show that the RS scheme outperforms the conventional private-information transmission approach. The gain is more significant in dense networks as well as in interference limited regimes. Besides, we show the benefits of joint clustering and RS mode design in enabling a better use of backhaul resources in C-RAN. This suggest RS-CMD techniques can improve the performance significantly in large and dense wireless networks.

## REFERENCES

- [1] A. A. Ahmad, H. Dahrouj, A. Chaaban, A. Sezgin, and M. Alouini, "Interference mitigation via rate-splitting in cloud radio access networks," in *2018 IEEE 19th International Workshop on Signal Processing Advances in Wireless Communications (SPAWC)*, June 2018, pp. 1–5.
- [2] J. G. Andrews, S. Buzzi, W. Choi, S. V. Hanly, A. Lozano, A. C. K. Soong, and J. C. Zhang, "What Will 5G Be?" *IEEE Journal on Selected Areas in Communications*, vol. 32, no. 6, pp. 1065–1082, June 2014.
- [3] L. B. Le, V. Lau, E. Jorswieck, N.-D. Dao, A. Haghighat, D. I. Kim, and T. Le-Ngoc, "Enabling 5G mobile wireless technologies," *EURASIP Journal on Wireless Communications and Networking*, vol. 2015, no. 1, p. 218, Sep 2015. [Online]. Available: <https://doi.org/10.1186/s13638-015-0452-9>



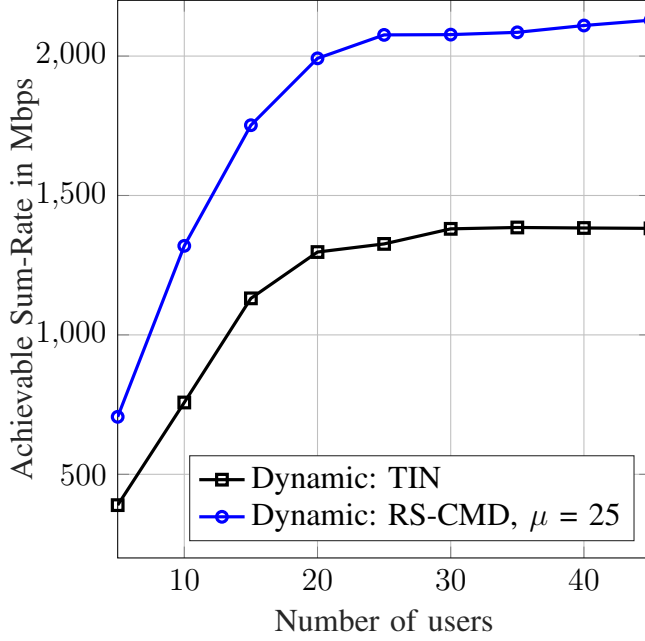


Figure 9: The achievable sum-rate, using dynamic RS-CMD with  $\mu = 25$  and dynamic TIN for the scenario in which a C-RAN with 7 BSs serving 28 users. Each BS has 4 Antenna. The inter-cell distance is 200 m

- [4] N. Bhushan, J. Li, D. Malladi, R. Gilmore, D. Brenner, A. Damnjanovic, R. T. Sukhavasi, C. Patel, and S. Geirhofer, "Network densification: the dominant theme for wireless evolution into 5g," *IEEE Communications Magazine*, vol. 52, no. 2, pp. 82–89, February 2014.
- [5] D. Wubben, P. Rost, J. S. Bartelt, M. Lalam, V. Savin, M. Gorgoglione, A. Dekorsy, and G. Fettweis, "Benefits and Impact of Cloud Computing on 5G Signal Processing: Flexible centralization through cloud-RAN," *IEEE Signal Processing Magazine*, vol. 31, no. 6, pp. 35–44, Nov 2014.
- [6] O. Simeone, A. Maeder, M. Peng, O. Sahin, and W. Yu, "Cloud radio access network: Virtualizing wireless access for dense heterogeneous systems," *Journal of Communications and Networks*, vol. 18, no. 2, pp. 135–149, April 2016.
- [7] Y. Shi, J. Zhang, and K. B. Letaief, "Group Sparse Beamforming for Green Cloud-RAN," *IEEE Transactions on Wireless Communications*, vol. 13, no. 5, pp. 2809–2823, May 2014.
- [8] M. Peng, C. Wang, V. Lau, and H. V. Poor, "Fronthaul-constrained cloud radio access networks: insights and challenges," *IEEE Wireless Communications*, vol. 22, no. 2, pp. 152–160, April 2015.
- [9] J. Tang, W. P. Tay, and T. Q. S. Quek, "Cross-layer resource allocation with elastic service scaling in cloud radio access network," *IEEE Transactions on Wireless Communications*, vol. 14, no. 9, pp. 5068–5081, Sep. 2015.
- [10] M. Tao, E. Chen, H. Zhou, and W. Yu, "Content-centric sparse multicast beamforming for cache-enabled cloud RAN," *IEEE Transactions on Wireless Communications*, vol. 15, no. 9, pp. 6118–6131, Sep. 2016.

- [11] Y. Ugur, Z. H. Awan, and A. Sezgin, "Cloud radio access networks with coded caching," *WSA 2016; 20th International ITG Workshop on Smart Antennas.*, pp. 1–5, March 2016.
- [12] A. Alameer and A. Sezgin, "Joint beamforming and network topology optimization of green cloud radio access networks," in *2016 9th International Symposium on Turbo Codes and Iterative Information Processing (ISTC)*, Sep. 2016, pp. 375–379.
- [13] A. Alameer and A. Sezgin, "Resource cost balancing with caching in C-RAN," *2017 IEEE Wireless Communications and Networking Conference (WCNC)*, pp. 1–6, March 2017.
- [14] A. Carleial, "Interference Channels," *IEEE Transactions on Information Theory*, vol. 24, no. 1, pp. 60–70, January 1978.
- [15] T. Han and K. Kobayashi, "A new achievable rate region for the interference channel," *IEEE Transactions on Information Theory*, vol. 27, no. 1, pp. 49–60, January 1981.
- [16] R. H. Etkin, D. N. C. Tse, and H. Wang, "Gaussian interference channel capacity to within one bit," *IEEE Transactions on Information Theory*, vol. 54, no. 12, pp. 5534–5562, Dec 2008.
- [17] A. Chaaban and A. Sezgin, "The Approximate Capacity Region of the Symmetric  $K$ -User Gaussian Interference Channel With Strong Interference," *IEEE Transactions on Information Theory*, vol. 62, no. 5, pp. 2592–2621, May 2016.
- [18] O. Simeone, O. Somekh, H. V. Poor, and S. Shamai (Shitz), "Downlink multicell processing with limited-backhaul capacity," *EURASIP Journal on Advances in Signal Processing*, vol. 2009, no. 1, p. 840814, Jun 2009.
- [19] S. Park, O. Simeone, O. Sahin, and S. Shamai, "Joint precoding and multivariate backhaul compression for the downlink of cloud radio access networks," *IEEE Transactions on Signal Processing*, vol. 61, no. 22, pp. 5646–5658, Nov 2013.
- [20] R. Zakhour and D. Gesbert, "Optimized Data Sharing in Multicell MIMO With Finite Backhaul Capacity," *IEEE Transactions on Signal Processing*, vol. 59, no. 12, pp. 6102–6111, Dec 2011.
- [21] B. Dai and W. Yu, "Sparse beamforming and user-centric clustering for downlink cloud radio access network," *IEEE Access*, vol. 2, pp. 1326–1339, 2014.
- [22] L. Liu and W. Yu, "Cross-layer design for downlink multihop cloud radio access networks with network coding," *IEEE Transactions on Signal Processing*, vol. 65, no. 7, pp. 1728–1740, April 2017.
- [23] H. Dahrouj and W. Yu, "Multicell interference mitigation with joint beamforming and common message decoding," *IEEE Transactions on Communications*, vol. 59, no. 8, pp. 2264–2273, August 2011.
- [24] O. Sahin, J. Li, Y. Li, and P. J. Pietraski, "Interference mitigation via successive cancellation in heterogeneous networks," in *2011 8th International Symposium on Wireless Communication Systems*, Nov 2011, pp. 720–724.
- [25] E. Che, H. D. Tuan, H. H. M. Tam, and H. H. Nguyen, "Successive interference mitigation in multiuser MIMO channels," *IEEE Transactions on Communications*, vol. 63, no. 6, pp. 2185–2199, June 2015.
- [26] Y. Mao, B. Clerckx, and V. O. K. Li, "Rate-splitting for downlink multi-user multi-antenna systems: Bridging NOMA and conventional linear precoding," *EURASIP Journal on Wireless Communications and Networking*, 2018.
- [27] Y. Mao, B. Clerckx and V. O. K. Li, "Energy Efficiency of Rate-Splitting Multiple Access, and Performance Benefits over SDMA and NOMA," in *2018 15th International Symposium on Wireless Communication Systems (ISWCS)*, Aug 2018, pp. 1–5.
- [28] Y. Mao, B. Clerckx, and V. O. K. Li, "Rate-splitting for multi-antenna non-orthogonal unicast and multicast transmission," in *2018 IEEE 19th International Workshop on Signal Processing Advances in Wireless Communications (SPAWC)*, June 2018, pp. 1–5.
- [29] E. Karipidis, N. D. Sidiropoulos, and Z. Luo, "Quality of service and max-min fair transmit beamforming to multiple cochannel multicast groups," *IEEE Transactions on Signal Processing*, vol. 56, no. 3, pp. 1268–1279, March 2008.
- [30] H. Dahrouj and W. Yu, "Coordinated beamforming for the multicell multi-antenna wireless system," *IEEE Transactions on Wireless Communications*, vol. 9, no. 5, pp. 1748–1759, May 2010.

- [31] D. Gesbert, S. Hanly, H. Huang, S. S. Shitz, O. Simeone, and W. Yu, "Multi-cell MIMO cooperative networks: A new look at interference," *IEEE Journal on Selected Areas in Communications*, vol. 28, no. 9, pp. 1380–1408, December 2010.
- [32] W. Yu, T. Kwon, and C. Shin, "Multicell coordination via joint scheduling, beamforming and power spectrum adaptation," in *2011 Proceedings IEEE INFOCOM*, April 2011, pp. 2570–2578.
- [33] D. W. H. Cai, T. Q. S. Quek, and C. W. Tan, "Coordinated max-min SIR optimization in multicell downlink - duality and algorithm," in *2011 IEEE International Conference on Communications (ICC)*, June 2011, pp. 1–6.
- [34] Y. Huang, C. W. Tan, and B. D. Rao, "Joint beamforming and power control in coordinated multicell: Max-min duality, effective network and large system transition," *IEEE Transactions on Wireless Communications*, vol. 12, no. 6, pp. 2730–2742, June 2013.
- [35] N. Naderializadeh and A. S. Avestimehr, "ITLinQ: A new approach for spectrum sharing in device-to-device communication systems," *IEEE Journal on Selected Areas in Communications*, vol. 32, no. 6, pp. 1139–1151, June 2014.
- [36] X. Wu, S. Tavildar, S. Shakkottai, T. Richardson, J. Li, R. Laroia, and A. Jovicic, "FlashLinQ: A synchronous distributed scheduler for peer-to-peer ad hoc networks," *IEEE/ACM Transactions on Networking*, vol. 21, no. 4, pp. 1215–1228, Aug 2013.
- [37] X. Yi and G. Caire, "Optimality of treating interference as noise: A combinatorial perspective," *IEEE Transactions on Information Theory*, vol. 62, no. 8, pp. 4654–4673, Aug 2016.
- [38] E. Chen and M. Tao, "Backhaul-constrained joint beamforming for non-orthogonal multicast and unicast transmission," in *GLOBECOM 2017 - 2017 IEEE Global Communications Conference*, Dec 2017, pp. 1–6.
- [39] A. A. Nasir and H. D. Tuan and T. Q. Duong and H. V. Poor, "Secure and energy-efficient beamforming for simultaneous information and energy transfer," *IEEE Transactions on Wireless Communications*, vol. 16, no. 11, pp. 7523–7537, Nov 2017.
- [40] S. Boyd and L. Vandenberghe, *Convex Optimization*. Cambridge University Press, 2004.
- [41] G. Scutari, F. Facchinei, and L. Lampariello, "Parallel and Distributed Methods for Constrained Nonconvex Optimization Part I: Theory," *IEEE Transactions on Signal Processing*, vol. 65, no. 8, pp. 1929–1944, April 2017.
- [42] M. S. Lobo, L. Vandenberghe, S. Boyd, and H. Lebre, "Applications of second-order cone programming," *Linear Algebra and its Applications*, vol. 284, no. 1, pp. 193 – 228, 1998, international Linear Algebra Society (ILAS) Symposium on Fast Algorithms for Control, Signals and Image Processing. [Online]. Available: <http://www.sciencedirect.com/science/article/pii/S0024379598100320>